2014 International Conference on Unmanned Aircraft Systems (ICUAS)
May 27-30, 2014. Orlando, FL, USA

Design and Manufacturing of a High Speed Jet Powered UAV

Ender Özyetiş
Aselsan Inc., Ankara, Turkey

Nafiz Alemdaroğlu
Department of Aerospace Engineering
Middle East Technical University, Ankara, Turkey

Abstract—**This paper presents the design and manufacturing of a high speed jet powered UAV which is capable of flying at M=0.5. Flight time of the UAV is 30 minutes at 1700 m above sea level. Aerodynamic and structural design of the UAV is conducted for 6g sustained and 9g instantaneous loads. Low aspect ratio blended wing-body design is decided due to low drag and high maneuverability. Structure of the UAV consists of the composite parts such as frames and skin and mechanical parts such as landing gears which are from aluminum and steel, engine holders, parachute release mechanism and etc.**

I. INTRODUCTION

The purpose of the study is to design and build a jet powered aircraft to be used as a target drone or a multi mission aircraft. Maximum speed is decided to be M=0.5 with a flight time of 30 minutes at 1700 m above sea level. Initial study is conducted by developing a design tool which works in an input-output way. Input parameters are categorized as blended wing-body parameters, tail parameters, propulsion system parameters, mission profile parameters, landing gear and parachute parameters, air properties and sample structural weights. Performance calculations are conducted by introducing an iterative weight calculation method. The Optimization process is conducted around the initial design by using the initial design parameters as a starting point. Some of the design inputs are selected as variable design parameters to construct the design cases which are formed via the combination of these variables. After final design is decided, modeling of the external geometry and modeling and integration of the sub-systems are conducted. Production is conducted in a step by step process which starts with the manufacturing of the skin pieces and frames and continues with joining of the structural parts prior to surface fibering and integration.

During the conceptual design, the UAV is decided to have a low aspect ratio and slender wing-body geometry due to the high aerodynamic and structural performance. The blended wing-body geometry is considered as a combination of the main wing and the front wing which is called as LEX. For the iterative weight calculations the longitudinal sections of the wing-body are assumed to be in the form of the wing airfoil and the span-wise sections are assumed to be in the form of diamond heights of which are determined by the airfoil upper and lower surface splines which are generated from the airfoil coordinates. Control surfaces are designed as elevons which are used as the elevator and ailerons at the same. The tail is considered as a passive surface which doesn't have any control surfaces but provides stability. The propulsive unit of the aircraft is selected as a mini turbojet engine which is capable of giving a 230 N thrust at sea level. The weight of the engine 1.5 kg and has a fuel consumption of 600 gram/minute at full throttle. The engine is controlled by an electronic control unit which controls the fuel flow through the engine.

Similar aircrafts which are used as target drones are investigated to have knowledge about the current status of this type of UAVs. Target drones are unmanned air vehicles which can be used for different type of missions, including: simulating enemy threats for gunnery and missile training, testing of new weapons such as air-to-air or surface-to-air missiles and pilot training such as air-to-air combat. Critical design criteria for the target drones can be considered maneuverability and speed. High cost sophisticated drones are made as re-usable/recoverable while some are directly hit and destroyed during the tests. Target drones are installed with electronic equipments such as active and passive radar systems, scoring systems and smoke systems. Due to the high speed necessity, turbojet engines are the most common propulsive units of this type of UAVs. Similarly, low aspect ratio small wings are general wing configurations. Catapult launch and parachute recovery are often seen for these aircraft which can be also assisted with rockets during take-off due to high wing loading and high takeoff speed.CEI Firejet [1], AAA Phoenix [2] and Adcom Yabhon HMD [3] are some of the platforms which can be considered as competitors. Weight of these platforms varies from 55kg to 220kg and maximum velocities vary from 550km/h to 800km/h. Table 1shows the similar aircrafts and their main specifications. These platforms have conventional fuselage and wing configuration. Instead of a conventional design, a different, more aerodynamic configuration which consists of blended wing-body and front leading edge extensions which are used as vortex generators is decided.

978-1-4799-2376-2/14/$31.00 ©2014 IEEE

Table 1. Specifications of Similar UAVs

CEI Firejet	
Weight (kg)	MTOW 150
Wing Span (m)	2
Length (m)	3.3
Max. Speed (m/s)	241
Endurance (min.)	60
Maneuverability	6g sustained, 10g instantaneous

AAA-Phoenix	
Weight (kg)	55
Wing Span (m)	2
Length (m)	2.4
Max. Speed (m/s)	154
Endurance (min.)	Up to 90

ADCOM-Yahbon HMD	
Weight (kg)	220
Wing Span (m)	3.38
Length (m)	4.32
Max. Speed (m/s)	222
Endurance (min.)	60

II. DEVELOPING THE DESIGN TOOL

Design and analysis process is integrated by introducing an input-output analysis method. Input design parameters are categorized as geometric parameters of wing and tail surfaces, mission profile parameters including take-off height and desired cruise time, landing gear parameters such as maximum allowable normal force during landing , propulsive unit parameters such as maximum thrust available and number of engines to be used and composite structure sample weights. Necessary look-up tables are generated for analysis process which includes variation of thrust coefficient of the engine over the mission profile and variation of maximum fuselage height that is derived from airfoil coordinates. Performance calculations are conducted by presenting an iterative detailed weight calculation method which gives more appropriate results than the conventional weight estimation methods that are generally based on historical data. The weights of structural parts such as frames and aircraft skin have been generated by using the composite structure sample weights together with the necessary design inputs. Necessary fuel weight, the landing gear and parachute weights have been generated iteratively to satisfy the selected design parameters. Figure 1 shows the design methodology.

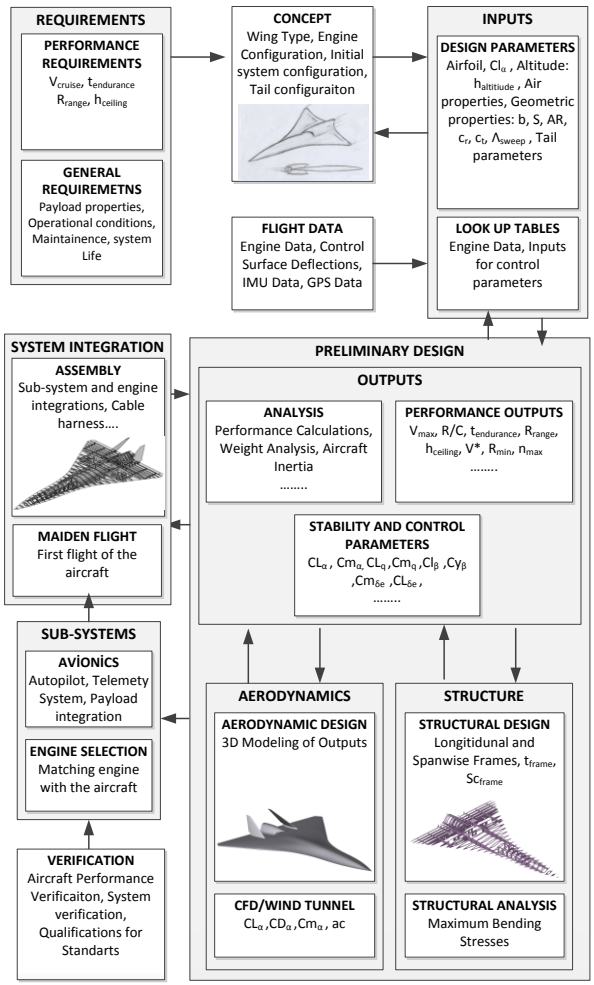

Figure 1. Design methodology

The design process is conducted by developing a tool which reads the input file consisting of the necessary design parameters for the analysis and gives the outputs. The input file is an Excel file in which the design parameters such as cruise speed, wing span, wing root and tip chord and etc. are stored. Sample composite material unit weights are also considered as inputs. Performance calculations are made by an iterative weight calculation method. Following sections include detailed information about the process. Figure 2 shows the method, basically.

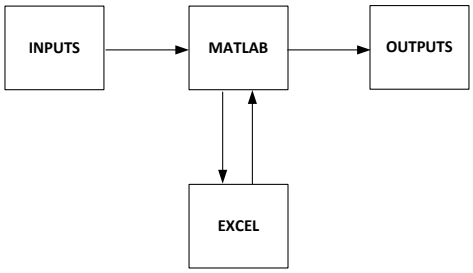

Figure 2. Basic design tool methodology.

Performance calculations are made on the Excel file while the read and write loops are coded into the Matlab script file. At each step the input parameters are assigned to the related cells in the Excel file and the outputs are read from the related cells. The steps are repeated for the number of designs.

A. Geometric Model

The geometry of the aircraft is determined by using the wing-body design parameters. Wing planform is assumed to be in the form of a delta wing combined with a front wing which is called as LEX (Leading Edge Extension) in this paper. The selection of the wing-body design parameters may cause positive sweep angles at the leading edge and positive or negative sweep angles at trailing edge, together. Total wing area is the sum the front wing area and the main wing area.

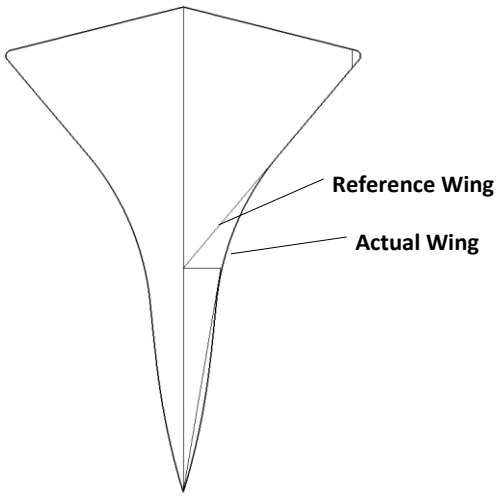

Figure 3. Reference and the actual wing

The structure of the aircraft is assumed such that it consists of internal frames which are located according to the given parameters and the aircraft skin. The parameterization is made for the frames which are generated automatically during the analysis for each design case. The aim of this process is to relate the change of aircraft geometry with the weight calculation. As a result, a better weight calculation can be obtained.

The longitudinal sections are assumed to be in the shape of the wing airfoil due to the fact that the aircraft is a blended wing- body design. The airfoil coordinates are read from the airfoil text file. The upper and lower airfoil splines are generated by the curve fitting method by using the coordinates of the airfoil.

The span-wise sections are assumed to be in the shape of diamonds for the ease of formulation. The heights of the diamonds are determined from the $y\left(\frac{x}{c}\right)$ function derived from airfoil data for the related x positions and the widths of the diamonds are determined from the span-wise length of the geometry at the x positions.

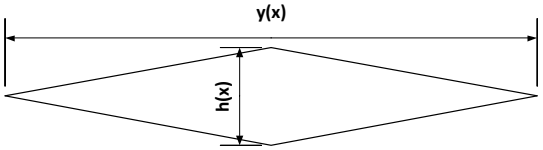

Figure 4. The diamond properties.

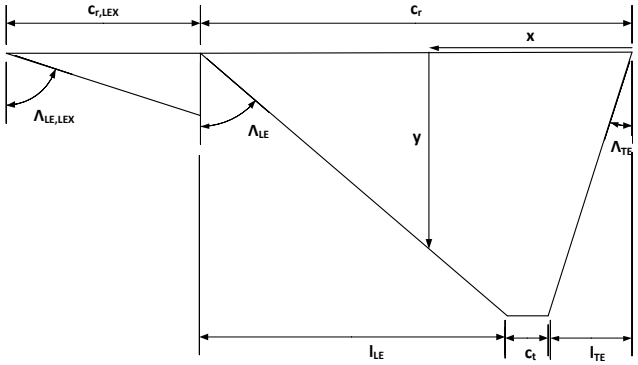

Figure 5. The longitudinal and spanwise section parameters

From Figure 4 and Figure 5;

$\boldsymbol{h(x) = y\left(\frac{x}{c}\right)\Big|_{upper} - y\left(\frac{x}{c}\right)\Big|_{lower}}$ and the $y(x)$ are determined as follows;

For the $\boldsymbol{x < l_{TE}}$, where $l_{TE} = \left(\frac{b}{2}\right) \cdot \tan(\Lambda_{TE})$;

$$y = \frac{tan\ (\Lambda_{TE})}{x} \tag{1}$$

For the $\boldsymbol{l_{TE} < x < l_{TE} + c_t}$,

$$y = b \tag{2}$$

For the $\boldsymbol{l_{TE} + c_t < x < c_r}$,

$$y = \frac{c_r - x}{tan\ (\Lambda_{LE})} \tag{3}$$

For the $\boldsymbol{c_r < x < c_r + c_{r,LEX}}$,

$$y = \frac{c_r + c_{r,LEX} - x}{tan\,(\Lambda_{LE,LEX})} \quad (4)$$

Figure 6 shows the initial conceptual and the actual frame sections. Conceptual frame sections are generated by the method described previously. Span-wise sections are in the diamond shape and the longitudinal ones in the form of the airfoil. Conceptual frame sections will be used to calculate frame section area. Although the actual wing shape is different from the conceptual one, this model is adequate to generate the weight distribution for the internal structure during the calculations.

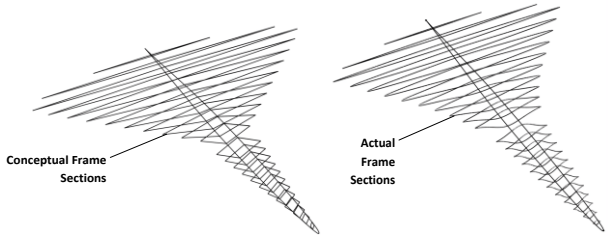

Figure 6. Initial conceptual and actual frame sections

B. Weight Model

During the conceptual design phase the weight estimation is the first step through the performance calculations. The conventional weight calculation method is based on the historical data which are obtained from the previously built commercial or military aircraft. Several constants are taken for each mission profile segment and the total weight is estimated. Instead of conventional method which can be inadequate for small unmanned aircraft, a detailed weight build-up method is used for the weight calculation. The weight of each component of the aircraft is calculated by using the design weight inputs. The frame and skin weight is calculated by using the sample unit weights for the frame and skin and the values generated from the geometric model calculations. The avionic weights are considered as an input. The fuel weight, landing gear weight, the parachute weight and the fuel tank weight are calculated iteratively. The fuel weight is calculated by running the mission profile for the initial weight guess which also includes the fuel weight. When the values are converged, the total weight is generated. This process is done on the Excel file for the design inputs sent from the Matlab code. Figure 7 shows the weight model, basically.

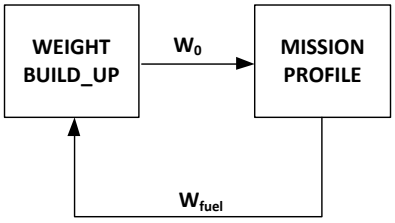

Figure 7. Iterative calculation of total weight

The weight analysis is one of the key steps in the calculation method described in this paper. As mentioned before the weight calculation is conducted in an iterative process. The fuel weight is the output of the mission profile analysis, but the mission profile analysis starts with the total weight value which also includes the fuel weight. So, it needs an iterative calculation. The reason of doing this is the fact the conventional weight estimation methods which relies on the historical data is not satisfactory for the small scale UAVs. So, more accurate iterative weight estimation is presented in this paper. Below the summary of the weight summation is given in Table 2.

Table 2. The Weight Build-up

#	Unit	#	Unit
1	W_{wing_skin}	12	W_{fuel}
2	W_{sp_frame} (span-wise frames)	13	$W_{engines}$
3	W_{lng_frame} (longitudinal frames)	14	W_{engine_comp}
4	W_{in_frame} (inlet frames)	15	$W_{main\_l\_gear}$
5	W_{frame} (2+3+4)	16	$W_{nose\_l\_gear}$
6	$W_{blended\_wing}$ (1+5)	17	$W_{avionics}$
7	W_{inlet}	18	$W_{batteries}$
8	W_{paint}	19	$W_{parachute}$
9	W_{wing_body} (6+7+8)	20	$W_{sys\_internal}$ (13+14+15+16+17+18+19)
10	W_{tail}	21	$W_{payload}$
11	W_{empty} (9+10+20)	22	$\boldsymbol{W_{TOTAL}}$ (11+12+21)

Total weight is calculated by summing up the structural weights and the internal component weights such as engine and fuel system, fuel, avionics, etc. The total weight is calculated as follows;

$$W_0 = W_{TOTAL} = W_{empty} + W_{fuel} + W_{payload} \quad (5)$$

Frame weights are calculated according to the conceptual frame section surface areas as described in Section II.A. The conceptual frames are multiplied with a fill ratio parameter which accounts for the gaps on the frame sections. The sample laminate weight is used to calculate the local frame weight.

The total frame weight is the sum of span-wise frames, longitudinal frames and inlet frames.

$$W_{frame} = W_{sp\_frame} + W_{lng\_frame} + W_{in\_frame} \quad (6)$$

For $\boldsymbol{N_{sp\_f}}$ number of span-wise frames, the total span-wise frame weight;

$$W_{sp\_frame} = \sum_{i=1}^{N_{sp\_f}} W_{sp\_frame}(i) \quad (7)$$

The local frame weight;

$$W_{sp\_frame}(i) = S_{sp\_frame}(i) \cdot W_{s_{frame}} \cdot F_{fill}(i) \quad (8)$$

$F_{fill}(i)$ is the fill ratio constant for the frames and $W_{s_{frame}}$ is the sample structural weight input for the frame in the units of gr/m^2.

Local frame areas are calculated by using the method described in Section II.A. Figure .8 shows the location of the diamonds. The calculation of the diamond areas is as follows;

For the $\boldsymbol{x(i) < l_{TE}}$, where $l_{TE} = \left(\frac{b}{2}\right) \cdot \tan(\Lambda_{TE})$;

$$S_{sp\_frame}(i) = \frac{\tan(\Lambda_{TE})}{x(i)} \cdot \frac{h(i)}{2} \quad (9)$$

For the $\boldsymbol{l_{TE} < x(i) < l_{TE} + c_t}$,

$$S_{sp\_frame}(i) = b \cdot \frac{h(i)}{2} \quad (10)$$

For the $\boldsymbol{l_{TE} + c_t < x(i) < c_r}$,

$$S_{sp\_frame}(i) = \frac{c_r - x(i)}{\tan(\Lambda_{LE})} \cdot \frac{h(i)}{2} \quad (11)$$

For the $\boldsymbol{c_r < x(i) < c_r + c_{r,LEX}}$,

$$S_{sp\_frame}(i) = \frac{c_r + c_{r,LEX} - x(i)}{\tan(\Lambda_{LE,LEX})} \cdot \frac{h(i)}{2} \quad (12)$$

The local positions are generated by the following function;

$$x(i) = \frac{c_r + c_{r,LEX}}{N_f + 1} \cdot (i) \quad (13)$$

The height of each frame from the equation in Section II.A;

$$h(i) = y\left(\frac{x(i)}{c}\right)\Big|_{upper} - y\left(\frac{x(i)}{c}\right)\Big|_{lower} \quad (14)$$

$\boldsymbol{c}$ is the chord length which is equal to $\boldsymbol{c_r + c_{r,LEX}}$ and the constants are the subtractions of the upper and lower surface function constants in this case. N_f is the number of frames.

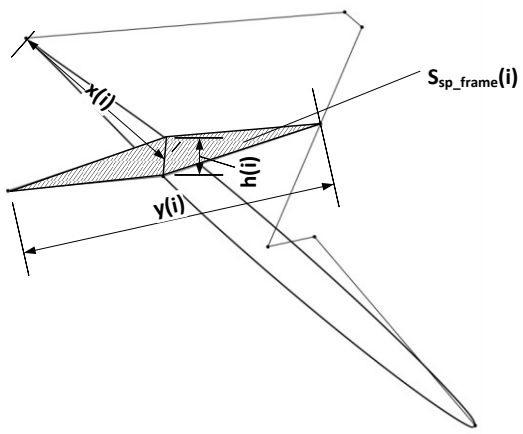

Figure .8 The location of the local frame

The areas of the longitudinal frames are calculated by taking the integral of $y\left(\frac{x}{c}\right)$ for upper and lower surfaces of the airfoil for different span-wise positions. The calculations are made for the main wing and the front wing separately.

$$W_{lng\_frame} = W_{mw\_lng\_frame} + W_{fw\_lng\_frame} \quad (15)$$

For the main wing;

For $\boldsymbol{N_{mw\_lng\_f}}$ number of longitudinal frames in main wing, the total frame weight;

$$W_{mw\_lng\_frame} = 2 \cdot \sum_{i=1}^{N_{mw\_lng\_f}} W_{mw\_lng\_frame}(i) \quad (16)$$

The reason of multiplying by two is the fact that longitudinal frames are symmetrical.

The local frame weight;

$$W_{mw\_lng\_frame}(i) = S_{mw\_lng\_frame}(i) \cdot W_{s_{frame}} \cdot F_{fill}(i) \quad (17)$$

$F_{fill}(i)$ is again fill ratio constant for the longitudinal frames.

The area of the longitudinal frames;

$$S_{mw\_lng\_frame}(i) = [c(i)]^2 \cdot \left(\int_0^{\frac{x}{c}} h(i)\Big|_{upper} - \int_0^{\frac{x}{c}} h(i)\Big|_{lower}\right) \quad (18)$$

The chord length of the local longitudinal frame;

$$c(i) = c_r - y(i) \cdot tan(\Lambda_{TE}) - y(i) \cdot tan(\Lambda_{LE}) \quad (19)$$

For the front wing;

For $\boldsymbol{N_{fw\_lng\_f}}$ number of longitudinal frames in front wing, the total frame weight;

$$W_{fw\_lng\_frame} = 2 \cdot \sum_{i=1}^{N_{fw\_lng\_f}} W_{fw\_lng\_frame}(i) \quad (20)$$

The chord length of the local longitudinal frame;

$$c(i) = c_{r,LEX} - y(i) \cdot \tan(\Lambda_{LE,LEX}) \quad (21)$$

$y(i)$ is the spanwise position of each longitudinal frame.

The weight of inlet frame is calculated by assuming the inlet section circular. The circular frames are multiplied by local fill ratio value and the weight is calculated.

For $\boldsymbol{N_{in\_f}}$ number of inlet frames, the total inlet frame weight;

$$W_{in\_frame} = \sum_{i=1}^{N_{in\_f}} W_{in\_frame}(i) \quad (22)$$

The local inlet frame weight;

$$W_{in\_frame}(i) = S_{in\_frame}(i) \cdot W_{s_{frame}} \cdot F_{fill}(i) \quad (23)$$

The area of the inlet frame;

$$S_{in\_frame}(i) = \pi \cdot (R_{inlet})^2 \quad (24)$$

The fuel weight, $\boldsymbol{W_{fuel}}$, is the output of the mission profile and calculated iteratively.

$$W_{fuel} = W_0 - W_7 \quad (25)$$

W_7 is the total weight at the end of the mission profile.

C. Defining The Design Cases

During the conceptual design the first design is determined. To find a better design, the calculations defined in previous sections are repeated for the number of designs. The important design input values are varied according to the specific limits which are selected around the first design values and matched with each other. So, for each match a different design is generated. The ones which do not satisfy the requirements are eliminated and the best design is selected.

The number of designs, $NOFD$, is determined as ;

$$NOFD = \prod_{i=1}^{Y_{inputs}} \left(X_{range}\right)_i \quad (26)$$

Where;
Y_{inputs} is the number of variable design inputs.
X_{range} is the range of each design input.

III. OPTIMIZATION

The optimization is conducted by using the initial design parameters as a starting point. Some of the design inputs are selected as variables and matched each other to form the different design cases.

The design variables the selected design inputs to construct the design cases. Each design case is formed via the combination of these design variables. Each design variable has a length which determined the size of the number of design parameter, NOFD.

The design parameters are selected as the main geometric parameters of the wing-body which is stated to be a combination of the main wing and the front wing which is called as LEX in this paper. The design variables are selected as in Table 3.

Table 3. The Variable Design Parameters

Parameter	Definition
c_r	Wing root chord
c_t	Wing tip chord
b	Wing span
Λ_{LE}	Wing leading edge sweep angle.
$c_{r,LEX}$	LEX root chord
b_{LEX}	LEX span

The design variables which are shown in Figure 9 determine the basic geometry of the main wing and the front wing. Instead of selected the wing loading or aspect ratio as design variables, the basic geometric parameters are considered as variables. So, in this method the wing loading and aspect ratio are generated according to the design variables.

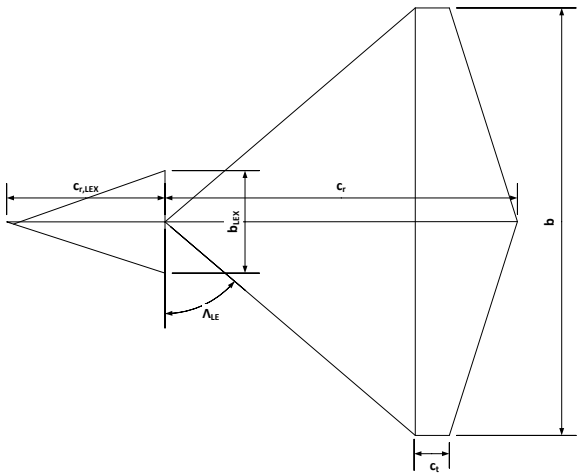

Figure 9. The design variables on the wing-body conceptual geometry.

The length of each design variable is determined by taking the initial design parameters as reference. So, the design variables are varied around the initial design parameters. The design parameters with length;

$c_r = [1.4\ 1.55\ 1.7]$
$c_t = [0.1\ 0.15\ 0.2]$
$b = [1.4\ 1.6\ 1.8]$
$\Lambda_{LE} = [50\ 60\ 70]$
$c_{r,LEX} = [0.8\ 0.96\ 1.2]$
$b_{LEX} = [0.3\ 0.4\ 0.5]$

Six variables have three different values. So, the number of designs from Equation 26;

$$NOFD = \prod_{i=1}^{Y_{inputs}} (X_{range})_i = \prod_{i=1}^{6} (X_{range})_i = 3^6 = 729$$

A. Results

After defining the constant and variable inputs for the analysis the optimization analysis is conducted. 729 designs are generated and elected according to the design requirements shown in Table 4.

Table 4. Design Selection Requirements

Requirement	Definition
$V_{max} \geq \mathbf{167\ m/s}$	Maximum speed at the operational altitude.
$t_{cruise} = \mathbf{30\ min}$	Cruise time.
$n_{max,sustained} \geq \mathbf{6}$	Maximum Sustained Load Factor.
$\Lambda_{TE} > \mathbf{0}^\circ$	Main Wing Trailing Edge Sweep Angle.
$V_{FUEL\,TANK} > \boldsymbol{V_{FUEL}}$	Fuel Tank Volume.

The design requirements are set to determine the limiting cases for the optimization analysis. The maximum speed is selected as 167 m/s at 1700m above the sea level which is selected as an input. The cruise time is a constant design input. All the design cases are generated for $t_{cruise} = 30$ min. The maximum sustained load factor is selected to be equal or greater than 6g's.

Some design requirements are set to check the geometry of the aircraft. The fuel tank volume constrain is necessarily is set to be bigger than the fuel volume calculated from the mission profile for a feasible design. The trailing edge sweep angle is selected to be a positive value which is required for a delta wing design.

Table 5 shows the satisfactory number of designs which are determined according to the design requirements. The available fuel tank constraint is satisfied by all the designs which is a result of the fuel tank design inputs which allows the usage of half of the wing span, thickness and mean chord for the fuel tank and the slender delta wing configuration which enables high internal wing volume. The most challenging constraint is the maximum sustained load factor. 21 designs are satisfactory for this constraint and all of the design constraints by the same time.

Table 5. The Satisfactory Number of Designs According to the Design Requirements

Design Constraint	Number of Satisfactory Designs
$V_{FUEL\,TANK} > V_{FUEL}$	729
$V_{max} \geq 167$ m/s	526
$\Lambda_{TE} > 0^\circ$	369
$n_{max,sustained} \geq 6$	21
ALL	21

As an initial election from the satisfactory designs, the design #30 due to the lowest weight and highest maximum velocity, the design #36, #63, #306 and #307 which have one of the highest total root wing-body chord which the summation of the main wing root chord and the LEX root chord and as a result thicker root section and design #57 for the highest load factor are selected.

Figure 10 shows the selected six wing configurations among the 21 satisfactory designs. Lowest weight and maximum velocity is achieved by the design #30 as a result of the smallest total wing-body area. All the satisfactory designs have a leading edge sweep angle of 50 degrees. Highest maximum load factor is achieved by the design #57.

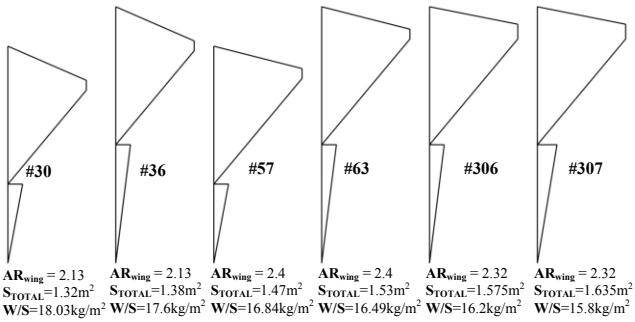

Figure 10. Selected wing-body configurations for the final election.

Longer wing-body root chord results in thicker wing-body root and more internal volume which is a desired property for such a slender, thin profile wing-body configuration. Although all of the designs have sufficient internal volume for the fuel, the designs which have longer root wing-body chord are selected over the others. As a result, design #30 and #57 which have the highest maximum velocity and load factor, respectively are eliminated. Final selection is conducted according to maneuver performance. Maximum load factor is considered as a selection criteria. The highest load factor is obtained by the design #63 among others. So, the final decision is made in favor of design #63.

The final design is selected as a result of the optimization process described in the previous section. The maximum velocity and maximum load factor are satisfied with the final design. Table 6 shows the comparison of the initial and final design according to some of the important design and performance parameters.

Table 6. Comparison of The Initial and Final Design

Parameters	Initial Design	Final Design
c_t [m]	0.2	0.1
c_r [m]	1.55	1.4
b [m]	1.6	1.8
Λ_{LE} [Deg.]	60	50
$c_{r,LEX}$[m]	0.96	1.2
b_{LEX}[m]	0.4	0.3
W_{TOTAL} [gr]	26304.3	25233.1
V_{fuel} [Litres]	9.97	9.21
$V_{FUEL\,TANK}$ [Litres]	17.64	15.6
V_{max} [m/s]	159.45	172.25
Λ_{TE} [Deg.]	0	14.18
$n_{max,sus.}$	4.21	6.29
S_{TOTAL} [m^2]	1.592	1.53
AR_{main_wing}	1.82	2.4
C_{L_α}	2.26	2.79
W/S	16.52	16.49
V_{stall} [m/s]	20.57	20.56
R/C [m/s]	44.95	50.17
$(R/C)_{max}$ [m/s]	45.18	51.33
V^* [m/s]	42.24	51.59
$R_{min,turn}$ [m]	44.4	43.64
$\omega_{max,turn}$ [Deg./s]	54.4	67.72
(T/W)	0.808	0.843
V_{cruise} [m/s]	87	87
$V_{R/C,max}$ [m/s]	92.25	99.4

As shown in Table 6, the maximum velocity and load factor design constraints are unsatisfactory for the initial design. The maximum velocity is $159.45\ \mathrm{m/s}$ and maximum load factor is 4.21. The total weight is 26304.3 grams for the initial design while the final design has a weight of 25233.1 grams which is less than the initial design. It means that design requirements are satisfied with a lighter design. The maneuvering capability is higher for the final design. The turn rate is increased from $54.4\ \mathrm{deg/s}$ to $67.72\ \mathrm{deg/s}$ and rate of climb is risen from $44.95\ \mathrm{m/s}$ to $50.17\ \mathrm{m/s}$.

B. Final Design Geometry

The wing body geometry, in chord-wise direction, is in the form of NACA 66 006 airfoil while in span-wise direction it is symmetrical diamond like shape.

The engine is located at the end of the aircraft due to the fact that the nozzle section of the engine contains high temperature mass flow and it means high heat signature for the infrared sensors. The infrared visibility of the aircraft is increased with this configuration. Another reason of locating engine to the back side is to protect structural parts of the aircraft against excessive heat.

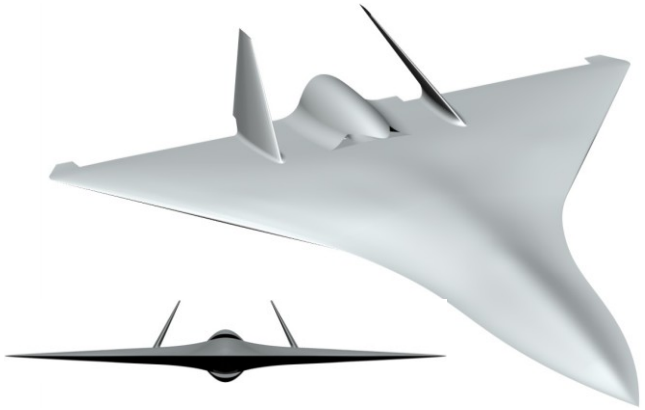

Figure 11. The Isometric and front view of the design (from top to bottom).

The side view is shown in Figure 12. The engine nozzle is outside of the structure of the aircraft.

Figure 12. The side view of the design.

The structure of the aircraft consists of the internal frames and the outer skin. Frames are made of Beech wood while the outer skin is made of balsa wood and fiber-glass and epoxy-resin combination. The internal frames are modeled according to the conceptual frames generated during the optimization process. The locations of the conceptual frames are taken as reference. Minor changes for the positions are made during the detailed design phase. Figure 13 shows the internal structure which consists of the span-wise and chord-wise frames and Figure 14 shows the inside of the UAV.

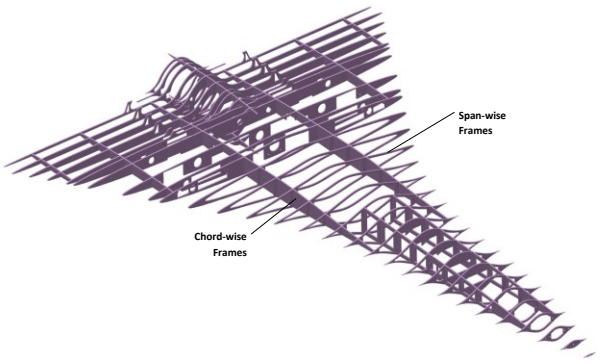

Figure 13. The Internal Structure.

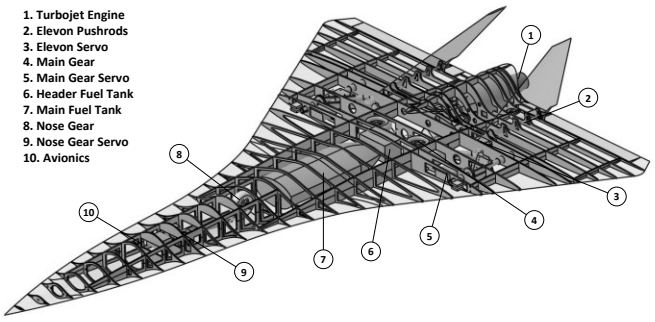

Figure 14. The inside of the UAV.

IV. PRODUCTION AND MAIDEN FLIGHT

Initial production is conducted for a scale version of the final design. The geometry of the aircraft together with the internal structures is scaled down to 1:2. The aircraft structure consists of span-wise and longitudinal frames and a skin which covers internal structure. Frames are produced from Beech plywood due to higher stiffness to weight ratio among other wood types. The skin is formed by covering the frames with 1mm Balsa wood which is properly shaped via a laser cutting process prior to the covering process. The outer layer of the skin is produced by covering the surface with fiberglass and resin to provide more stiffness. Figure 15 shows the production methodology basically.

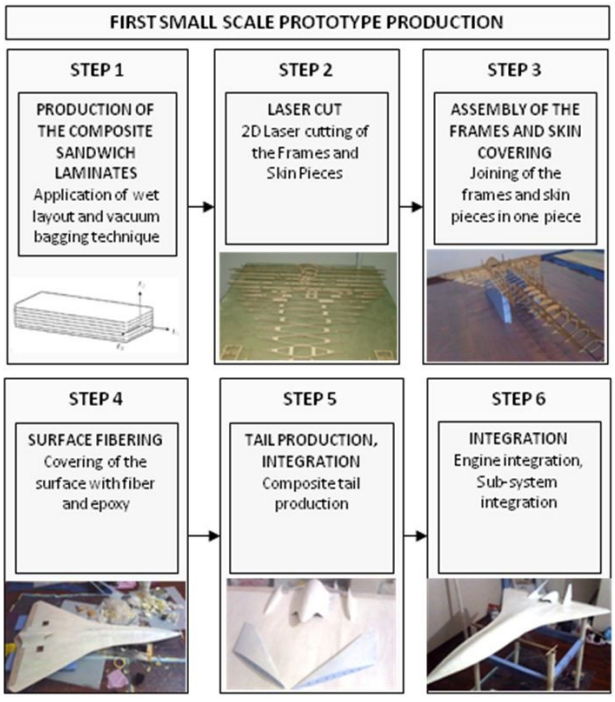

Figure 15. The Production Methodology

The maiden flight is conducted with the initial scaled prototype. The flight runway is located at Mamak in Ankara. Figure 16 and Figure 17 show some pictures during the flight day.

Figure 16. The initial prototype.

Figure 17. The initial prototype at maiden flight.

V.CONCLUSION

In this study design of a high speed target drone which is capable of flying at 0.5 Mach is conducted. Total flight time is set to 30 minutes. The engine is selected as a single turbojet engine which gives 230 N of thrust at sea level. The takeoff is performed on the runway while landing can be performed via parachute. Fuel tanks are located inside of the wing-body. Engine nozzle is located outside of the wing-body to increase the heat signature. Passive tail surfaces are inclined inwards for longitudinal stability. Control surfaces are selected as elevons.

The optimization process is conducted by assigning the each design case parameters to the corresponding cells in the Excel file and writing the results to a new file. The key point for optimization process is to find a good starting point since the optimization is conducted around the initial design parameters.

The total weight is heavily dependent on the cruise time input which forces the mission profile to generate the necessary fuel amount for the given input. Sample structural weights are considered as design inputs. In this thesis, the design methodology does not include structural modules to check whether the generated geometry is satisfactory for the pre-determined g loads or not. Instead, sample structural weight inputs which are determined experimentally prior to the design process are used to satisfy the structural stiffness.

To determine these inputs sample structures are built and checked whether they are satisfactory for the desired g loads prior to the final design.

Production is started with 3D modeling of the aircraft. The skin is divided into pieces and unfolded for the 2D laser cut process. Wooden panels are used to produce the internal frames. During the assembly of the frames the positioning is important to eliminate shifting of the frames. So, the longitudinal frames are fixed by using a fixture which is produced according to the longitudinal frame geometry.

Maiden flight is performed with the initial design scaled prototype. The scale factor is determined to be 1:2. The high maneuvering capability of the UAV is observed during the flight. The longitudinal stability of the aircraft is observed as satisfactory.

As a future work following remarks are determined;

- The scale version of the final design is planned with the integration of the turbojet engine.
- The verification of the performance parameters such as maximum speed, cruise time and maneuvering capability is supposed to be conducted.
- The deployment of avionics including the autopilot and radar systems may be done.
- The cruise time may be increased by removing the parachute option. Alternatively, landing gears may be removed by introducing the catapult lunch and parachute recovery.
  - Thrust vectoring option may be considered to increase the maneuvering capability.
  - To increase the lifting performance a thicker airfoil may be selected.
  - The vertical tail area may be increased for better lateral stability.
  - Skin can be produced by using molds instead of covering the frames with pre-produced skin pieces.

REFERENCES

[1] CEI-Firejet,URL: http://www.cei.to/aerialtargetsystems/firejet.aspx, [cited March 2013]

[2] AAA Phoenix, URL: http://www.airaffairs.com.au/phoenix_jet.html, [cited March 2013]

[3] ADCOM Yabhon HMD , URL:http://adcom-systems.com/eng/Targets/YAHBON-HMD, [cited March 2013]

[4] Houghton, E.L. and Carpenter, P.W., Aerodynamics for Engineering Students, Butterworth-Heinermann, 2003.

[5] Roskam, Jan , Airplane Flight Dynamics And Automatic Flight Controls, Roskam Aviation and Engineering Corporation, 1979.

[6] Anderson, John D., Aircraft Performance and Design, McGraw-Hill, 1999

[7] Roskam, Jan , Tau Edward Lan, Dr. Chuan, Airplane Aerodynamics and Performance, DarCorporation, 1997.

[8] Roskam, Jan, Methods for Estimating Stability and Control Derivatives of Conventional Subsonic Airplanes, 1971.

[9] Roskam, Jan, Airplane Design-Part VI: Preliminary Calculation of Aerodynamic, Thrust and Power Characteristics, DARcorporation, 2000.

[10] Raymer, Daniel P., Aircraft Design: A conceptual Approach, AIAA, 1992.

[11] Abbott, Ira H., Theory of Wing Sections, Dover Publications, INC., 1959.

[12] Amt Netherlands, URL: http://www.amtjets.com, [cited May 2013].

[13] Schlichting, Hermann and Truckenbrodt, Erich, Aerodynamics of the Airplane, McGraw-Hill, 1979

[14] Özyetiş, E., "Design and Manufacturing of a High Speed-Jet Powered Target Drone", Thesis (MSc), Middle East Technical University, 2013.